

The Quantum Bohm Potential for Many-Fermion Systems

Zh. A. Moldabekov,^{1,2,*} T. Dornheim,^{1,2} G. Gregori,³ F. Graziani,⁴ M. Bonitz,⁵ and A. Cangi^{1,2,†}

¹Center for Advanced Systems Understanding (CASUS), D-02826 Görlitz, Germany

²Helmholtz-Zentrum Dresden-Rossendorf, D-01328 Dresden, Germany

³Department of Physics, University of Oxford, Parks Road, Oxford OX1 3PU, UK

⁴Lawrence Livermore National Laboratory, Livermore, CA, 94550, USA

⁵Institut für Theoretische Physik und Astrophysik,

Christian-Albrechts-Universität zu Kiel, Leibnizstraße 15, 24098 Kiel, Germany

Correlated many-fermion systems emerge in a broad range of phenomena in warm dense matter, plasmonics, and ultracold atoms. Quantum hydrodynamics (QHD) complements common first-principles methods for many-fermion systems and enables simulations at larger length and longer time scales. While the quantum Bohm potential is central to QHD, we illustrate its failure for strong perturbations. We extend QHD to this regime by utilizing the *many-fermion quantum Bohm potential*. This opens up the path to more accurate simulations in strongly perturbed warm dense matter, inhomogeneous quantum plasmas, and on nano-structure surfaces at scales unattainable with first-principles algorithms. The *many-fermion quantum Bohm potential* might also have important astrophysical applications in developing conformal-invariant cosmologies.

Correlated quantum many-fermion systems are currently in the focus of several fields ranging from high-energy-density physics [1] to ultracold fermionic atoms [2, 3], and correlated materials [4]. Progress in all these fields relies on accurate theory and simulations including quantum Monte Carlo (QMC) [5, 6], density functional theory (DFT) [7, 8], nonequilibrium Green functions [9, 10], and density matrix renormalization group (DMRG) methods [11]. While remarkable progress was achieved with these methods, their high computational cost and fundamental bottlenecks significantly restrict their application. For example, the fermion sign problem complicates the use of QMC [12, 13], or the computational cost of DMRG renders them infeasible in three spatial dimensions. Therefore, there is a high need for complementary methods that extend the domain of simulations to length and time scales relevant for experiments, even at the price of reduced accuracy [14].

One such method is quantum hydrodynamics (QHD). There has recently been a surge of activities in a number of research areas including warm dense matter (WDM) [14–24], plasmonics [25–33], electron transport in semiconductor devices and thin metal films [34–37], reactive scattering [38, 39], cosmology, and dark matter research [22, 40–46].

QHD complements aforementioned first-principles methods for quantum dynamics by enabling simulations at larger length and longer time scales [14, 20, 21]. The quantum Bohm potential is central to QHD [16, 18, 23, 24, 34, 35, 47]. It captures quantum tunneling, spill out, and other non-local effects. Commonly, the quantum Bohm potential is approximated as $v_B(\mathbf{r}, t) = -\hbar^2/(2m) [\nabla^2 \sqrt{n(\mathbf{r}, t)} / \sqrt{n(\mathbf{r}, t)}]$ in terms of the mean density of electrons $n(\mathbf{r}, t)$; hereafter called *standard Bohm potential*. It is utilized in this form to model phenomena in various many-fermion systems.

While standard QHD has proven useful for these phe-

nomena, we question the validity of v_B when strong density perturbations are present. These emerge in strongly perturbed WDM [48] and quantum plasmas [49, 50]. Most notably, this regime is probed in recent and upcoming X-Ray scattering measurements of matter that is shock-compressed and laser-excited [51–56] using the seeding technique discussed in the conclusions.

In this Letter, we therefore extend QHD to the regime of strong density perturbations considering WDM. Our central result is to utilize the *many-fermion quantum Bohm potential*

$$\tilde{v}_B(\mathbf{r}, t) = -\frac{\hbar^2}{2mN} \sum_{i=1} f_i \frac{\nabla^2 \sqrt{n_i(\mathbf{r}, t)}}{\sqrt{n_i(\mathbf{r}, t)}} \quad (1)$$

within QHD [18, 47], where N is the total number of electrons. Specifically, we (1) generate an exact *many-fermion quantum Bohm potential* based on *exact* QMC data, (2) show how the standard Bohm potential breaks down for strong density perturbations, and (3) highlight how key ingredients to QHD (forces) differ greatly in this regime. We exemplify this for the harmonically perturbed, interacting electron gas at finite temperature.

Utilizing the *many-fermion quantum Bohm potential* in QHD is motivated by the fact that it is derived from the exact quantum dynamics of electrons within TDDFT which provides the crucial link between QHD and interacting many-fermion systems [14].

Theory. We begin with the non-relativistic, many-particle Hamiltonian of interacting fermions

$$\hat{H} = \hat{T} + \hat{V}_{ee} + \hat{V}, \quad (2)$$

where \hat{T} denotes the kinetic energy operator, \hat{V}_{ee} the electron-electron interaction and \hat{V} the external potential including the ionic background. The solutions are N -particle wave functions that are antisymmetric and normalized. For the sake of clarity we consider only

spin-unpolarized systems. A formally exact and computationally feasible solution to the quantum dynamics of electrons is given within TDDFT. Here, a set of N time-dependent Kohn-Sham (KS) equations

$$i\hbar \frac{\partial}{\partial t} \phi_i(\mathbf{r}, t) = \left[-\frac{\hbar^2}{2m} \nabla^2 + v_s(\mathbf{r}, t) \right] \phi_i(\mathbf{r}, t), \quad (3)$$

yields the exact time evolution of the electronic density, $n(\mathbf{r}, t) = \sum_i f_i |\phi_i(\mathbf{r}, t)|^2$, in terms of the single-particle KS orbitals $\phi_i(\mathbf{r}, t)$, where f_i denotes an occupation function. This is achieved by the KS potential, $v_s(\mathbf{r}, t) = v(\mathbf{r}, t) + v_H[n](\mathbf{r}, t) + v_{xc}[n](\mathbf{r}, t)$, which exactly mimicks the electron-electron interaction within a mean-field description. Here, v denotes the external potential, $v_H[n]$ the classical electrostatic (Hartree) potential, and $v_{xc}[n]$ the exchange-correlation potential.

Now, the time-dependent KS equations are reformulated into a set of coupled QHD equations by the following steps [14, 23, 47]: (1) we insert the amplitude-phase representation of the KS orbitals [57–59], $\phi_i(\mathbf{r}, t) = \sqrt{n_i(\mathbf{r}, t)} \exp[iS_i(\mathbf{r}, t)]$, into the time-dependent KS equations; (2) we use the expression for the mean orbital density, $\bar{n}(\mathbf{r}, t) = \sum_i f_i n_i(\mathbf{r}, t)/N$, and velocity, $\mathbf{v} = \sum_i f_i \mathbf{v}_i/N$, where we introduce $n_i(\mathbf{r}, t) = |\phi_i(\mathbf{r}, t)|^2$, as the KS orbital density and $\mathbf{v}_i = \nabla S_i(\mathbf{r}, t)/m$, as the KS orbital velocity; (3) we introduce density and velocity fluctuations $n_i = \bar{n} + \delta n_i$ and $\mathbf{v}_i = \mathbf{v} + \delta \mathbf{v}_i$ [18, 23, 35, 47]. These steps yield the formally exact QHD equations

$$\frac{\partial \bar{n}}{\partial t} + \frac{1}{N} \sum_i f_i \nabla \cdot (n_i \mathbf{v}_i) = 0, \quad (4)$$

$$m \frac{\partial \mathbf{v}}{\partial t} = -\nabla \tilde{v}_B - \frac{1}{n} \nabla P_e + \frac{1}{n} \nabla \cdot \boldsymbol{\sigma}_e + e\mathbf{E} - \nabla v_{xc}, \quad (5)$$

where we have not yet made any assumptions about velocity and density fluctuations. In Eq. (5), e is the absolute value of the electron charge, $P_e = \frac{1}{2m} \partial_\alpha \overline{\delta p_{i\alpha}^2}$ the electronic pressure term (with $\delta \mathbf{p}_i = m \delta \mathbf{v}_i$), $\boldsymbol{\sigma}_e = \frac{1}{m} \partial_\gamma \overline{\delta p_{i\alpha} \delta p_{i\gamma}}$ with $\gamma \neq \alpha$ the electronic viscous stress-tensor, and $\mathbf{E} = -\nabla[v + v_H]$ the electric field due to the Hartree and external potentials. The first equation is the continuity equation, whereas the second is the momentum conservation equation. Notice that the *many-fermion quantum Bohm potential* emerges naturally. Also note that these QHD equations are equivalent to the time-dependent KS equations.

These QHD equations are turned into computationally feasible practice by employing approximations to (1) the exchange-correlation functional v_{xc} , (2) the equation of state P_e , (3) the viscous stress-tensor $\boldsymbol{\sigma}_e$, and (4) setting $\frac{1}{N} \sum_i f_i \nabla \cdot (n_i \mathbf{v}_i) = \nabla \cdot (\bar{n} \mathbf{v})$ in Eq. (4) where the averaged fluctuations of a flux $\langle \delta \mathbf{j} \rangle = \langle \delta n_i \delta \mathbf{v}_i \rangle$ are assumed to be negligible compared to the mean value $\mathbf{j} = \bar{n} \mathbf{v}$ [23, 24, 35, 47]. In particular, using approximations to the equation of state and the viscous stress-tensor enables QHD to go

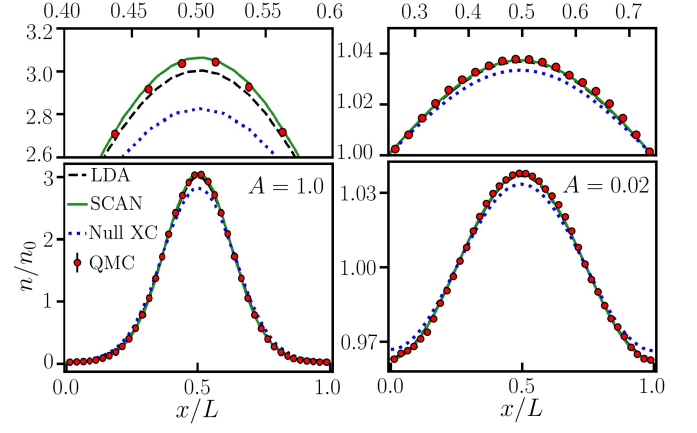


FIG. 1. Electronic density in the potential (6) for two different amplitudes A , at $r_s = 2$ and $\theta = 1$. QMC results (red circles) are compared to KS-DFT data for different XC-potentials: solid green: SCAN; dashed black: LDA; dotted blue: non-interacting fermions ($v_{xc} = 0$).

beyond the length and time scales that are attainable in TDDFT calculations [20–24, 27, 29].

Results. As the central result of this work we demonstrate the relevance of the *many-fermion quantum Bohm potential* in the set of QHD equations (4) and (5), whereas in all prior works the standard Bohm potential was used. First, we generate a *many-fermion quantum Bohm potential* using KS-DFT [60] based on exact QMC calculations of the harmonically perturbed, interacting electron gas. Then we show that the standard Bohm potential differs both qualitatively and quantitatively from \tilde{v}_B to a great extent for strong and moderate perturbations of the electron density. Finally, we illustrate how these deviations yield vastly different forces. We, hence, argue that these lead to a different quantum plasma dynamics when used in the QHD equations. Agreement to better than 50% in the resulting forces is achieved only for small density perturbations when $|\delta n| \lesssim 10^{-3} n_0$ or $q > 2q_F$. This is further analyzed in the Supplementary Material [61]. The use of the *many-fermion quantum Bohm potential* now renders QHD valid for the regime of strong density perturbations. While approximations to the pressure and viscous stress-tensor also influence the accuracy of the QHD equations, we focus on the *many-fermion quantum Bohm potential*. It primarily determines the accurate inclusion of quantum effects, e.g., tunneling and spill-out, crucial for the aforementioned applications [26–32, 49–56, 62].

We illustrate the significance of our result by considering the interacting electron gas subject to a harmonic external potential

$$v(\mathbf{r}) = 2A \cos(\mathbf{r} \cdot \mathbf{q}), \quad (6)$$

where we assume periodic boundary conditions and choose the x-axis along \mathbf{q} with $q = nq_{\min}$, $q_{\min} = 2\pi/L$,

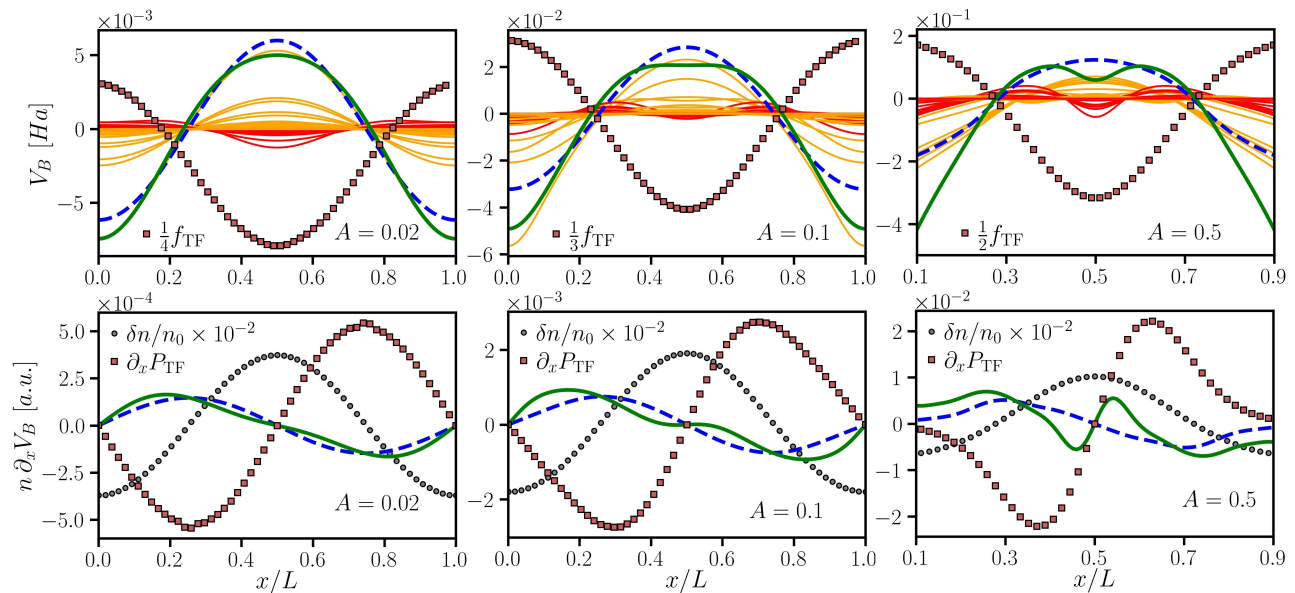


FIG. 2. Upper panel: Comparison of the exact *many-fermion quantum Bohm potential* (thick green) with the standard Bohm potential (dashed blue) at $r_s = 2$ and $\theta = 1$. Additionally, the TF free energy density (red squares, scaled) and the contributing KS orbitals (thin red (dark) and orange (light) lines) are illustrated. The contribution of orbitals is scaled by a factor two (three) at $A = 0.02$ ($A = 0.1$ and $A = 0.5$). Lower panel: Comparison of the forces from the *many-fermion quantum Bohm potential* (green) with forces from the standard Bohm potential (dashed blue). We also display the TF pressure (squares) and the density profile (grey circles). Note the scaling.

$L = (N/n_0)^{1/3}$, and n_0 the number density of electrons. By varying the amplitude A , the character of the KS orbitals changes from plane waves to strongly localized wave packets. Moreover, by varying both A and the wave number q , we tune the density gradients from small to large. The relevant parameter space is spanned by the density parameter $r_s = a/a_B$ and the degeneracy parameter $\theta = k_B T/E_F$, where a is the mean inter-electronic distance, a_B the first Bohr radius, T the temperature, and E_F the Fermi energy. For the remainder of this paper we choose $r_s = 2$ and $\theta = 1$. This corresponds to the WDM and quantum plasma regime [63–65].

The construction of the *many-fermion quantum Bohm potential* relies on accurate KS orbitals. We generate orbitals using KS-DFT for various amplitudes $10^{-3} \leq A \leq 1$ corresponding to the range from weak to strong perturbations. We assess their accuracy by comparing them with the exact result provided by QMC calculations [6, 66] (the computational details of both KS-DFT and QMC calculations are given in the Supplemental Material [61]). The obtained electronic densities for $A = 1$ and $A = 0.02$, using various exchange-correlation approximations (non-interacting fermions, LDA [60], and SCAN [67]) are illustrated in Fig. 1, where $q_{\min} = 0.84q_F$. The comparison with the QMC data (red circles) confirms that the KS-DFT calculations using the SCAN functional provide the KS orbitals that virtually yield the exact density.

As the next step, we now construct an exact *many-*

fermion quantum Bohm potential by inserting these KS orbitals into Eq. (1). The results are shown in the top panel of Fig. 2. They are ordered in increasing perturbation strength ($A = 0.02, 0.1, 0.5$). At the top we compare the *many-fermion quantum Bohm potential* (thick green) with the standard Bohm potential (dashed blue). We observe significant differences for all amplitudes, and a profound qualitative difference at high perturbation strength ($A = 0.5$). To better understand the origin of these differences, consider contributions of the individual KS orbitals with a maximum and a minimum in the central region (orange and red lines, respectively). The former lead to a stronger *many-fermion quantum Bohm potential* in the density depletion region at the edges, whereas the latter yield a weaker *many-fermion quantum Bohm potential* in the central region where electrons accumulate. The important point to note is that the contribution from individual orbitals does not depend on the amplitude of the orbital density, but on its shape as is apparent from Eq. (1). This means that the contribution of a highly curved orbital can be critical, even if the corresponding occupation number may be relatively small.

Next, we relate the observed differences to the relevant energy scale in the QHD equations. We compare against the ideal part of the free energy density, $f_{\text{TF}}[n(\mathbf{r})] = \delta F_{\text{id}}[n]/\delta n(\mathbf{r}) = \mu$ (red squares), which is a common approximation to the pressure in the QHD equations [23, 24, 34, 35] in terms of the Thomas-Fermi (TF) free-energy functional. The top panel of Fig. 2 shows that

the ideal part of the free energy density is of about the same order of magnitude as the quantum Bohm potential throughout highlighting the importance of the *many-fermion quantum Bohm potential* in the QHD equations.

Now we assess the impact of using the *many-fermion quantum Bohm potential*, instead of the standard Bohm potential, for simulating quantum dynamics within the QHD equations. We compute the force due to the pressure of a quantum Bohm potential from $n(\mathbf{r})\nabla V_B$, where V_B is either the standard Bohm potential v_B or the *many-fermion quantum Bohm potential* \tilde{v}_B . To assess the importance of the observed differences, we compare them with the force due to TF pressure, $\nabla P_{\text{TF}} = n(\mathbf{r})\nabla f_{\text{TF}}[n(\mathbf{r})]$. The lower panel of Fig. 2 demonstrates significant differences in the forces. At small perturbation strength the maximum deviation of the forces is already 50%. This deviation further increases with a stronger perturbation amplitude A . At $A = 0.5$, they differ substantially, and the standard expression fails to even yield a qualitative description. In the central region they are also qualitatively very different. Furthermore, the comparison with the TF force highlights the relative importance of the force due to \tilde{v}_B . At $A = 0.02$, the TF force is about four times stronger than the force due to both variants of the quantum Bohm potential. With increasing perturbation strength, the force due to the *many-fermion quantum Bohm potential* becomes more relevant. At $A = 0.5$, it is close to the TF force in the central region, whereas it even exceeds the TF force in the density depletion regions close to the edges.

Next, in Fig. 3, we provide a more detailed comparison of the forces. On the left we show the ratio of the forces due to the *many-fermion quantum Bohm potential* and the standard Bohm potential, respectively, whereas on the right we show the ratio of the force due to \tilde{v}_B with the TF force, at $A = 0.1, 0.3, 1.0$. We infer that, in general, the standard Bohm potential differs from the exact *many-fermion quantum Bohm potential* by at least a factor of two throughout (left panel). For a small perturbation amplitude, $A = 0.1$, the standard Bohm potential significantly overestimates (up to fifty times) the exact *many-fermion quantum Bohm potential* in the central region and underestimates it by a factor of two in the density depletion region. At larger amplitudes ($A = 0.3$ and $A = 1.0$), the differences in both the density depletion region and in the central region increase. Finally, in Fig. 3 (right), we assess the relative importance of the magnitude of the quantum Bohm potentials. We deduce that the force due to the *many-fermion quantum Bohm potential* is dominant in the density depletion regions, when $A \gtrsim 0.3$, with a maximum value of the density increase of $|\delta n| \gtrsim 0.6 n_0$.

Conclusion. For a degenerate quantum many-particle system with Bose statistics in the condensate, the Madelung decomposition leads to the Gross-Pitaevski equation. Here, the exactness of the standard Bohm po-

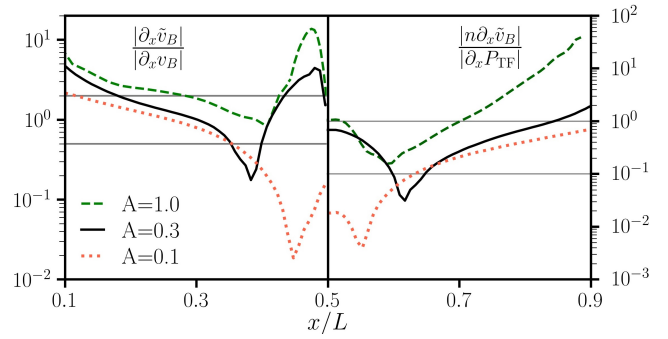


FIG. 3. Left: Ratio of the forces between the exact *many-fermion quantum Bohm potential* (\tilde{v}_B) and the standard Bohm potential (v_B) at $r_s = 2$ and $\theta = 1$ for increasing density perturbation amplitudes A . Right: Ratio of the forces due to the quantum Bohm potential, \tilde{v}_B , and the TF pressure.

tential can be proven [18]. For fermionic systems, such a proof does not exist. A trivial exception is the case when the amplitudes of all orbitals coincide and the system is mapped onto a single orbital [47].

In this work, we carried out the very first investigation of the quantum Bohm potential for a correlated many-fermion system based on first-principles data from QMC and KS-DFT. Despite its long history in quantum mechanics since its derivation by Bohm in 1952 [58] and its importance as a computational device in QHD, this has not been attempted before. Our key result highlights the very limited applicability of the standard Bohm potential which is used in virtually all previous works of QHD. We showed that it is only valid for a very weakly perturbed electron gas ($|\delta n| \lesssim 10^{-3} n_0$) or at very large wave-numbers ($q > 2 q_F$). Likewise, we demonstrated that the *many-fermion quantum Bohm potential* is needed to model nonlinear phenomena in quantum plasmas and WDM. We further illustrated the significance of the force produced by the *many-fermion quantum Bohm potential* in strongly inhomogeneous plasmas.

We anticipate that the *many-fermion quantum Bohm potential* will play a significant role for many upcoming experiments. Strongly perturbed WDM states are generated and probed, for example, using THz lasers with an intensity of 600 kV/cm that corresponds to a perturbation amplitude of $A \simeq 0.3$ [51] and using free electron lasers with intensities of up to 10^{22} W/cm² that lead to $A \approx 2$ [49]. Another exciting application of QHD is inertial confinement fusion [68–70] where strongly inhomogeneous electronic states emerge in the heating of shock-compressed fuel capsules. Of particular interest is the effect the Bohm pressure term has on the shock behavior in high-energy density applications using lasers or pulsed power. The presence of higher-order spatial derivatives of the density produces a dissipative-like effect on the shock structure, shearing the interface and broadening the shock front. Other interesting applications

include non-linear wave phenomena and instabilities in quantum plasmas [23, 24]. We also expect the *many-fermion quantum Bohm potential* to impact the field of nano-plasmonics [25–33] where simulations of large nano-clusters are routinely performed with QHD. Moreover, the *many-fermion quantum Bohm potential* might enable quantum dynamics simulations of cold atom experiments that study thermodynamic and transport properties [2, 3, 71]. We also speculate that the force field generated by the *many-fermion quantum Bohm potential* can be utilized as a computationally inexpensive neural-network surrogate model as it was done, e.g., for the free energy functional in KS-DFT [72, 73] and the local field correction in QMC [74, 75].

Finally, the *many-fermion quantum Bohm potential* awaits exciting applications in cosmology. These approaches are based on an observation made by de Broglie pointing out that quantum mechanical effects are entirely equivalent to a conformal transformation of the background metric [76, 77]. This leads to a representation of the non-local Bohm potential of all the particles in the Universe as an effective cosmological constant [40]. Therefore, this outlines an interesting line of future research.

ACKNOWLEDGMENTS

This work was partly funded by the Center for Advanced Systems Understanding (CASUS) which is financed by Germany’s Federal Ministry of Education and Research (BMBF) and by the Saxon Ministry for Science, Culture and Tourism (SMWK) with tax funds on the basis of the budget approved by the Saxon State Parliament. We gratefully acknowledge CPU-time at the Norddeutscher Verbund für Hoch- und Höchstleistungsrechnen (HLRN) under grant shp00026 and on a Bull Cluster at the Center for Information Services and High Performance Computing (ZIH) at Technische Universität Dresden. The work of GG was funded in parts by the Engineering and Physical Sciences Research Council (grant numbers EP/M022331/1 and EP/N014472/1) and AWE plc. MB acknowledges support from the Deutsche Forschungsgemeinschaft via grant BO1366/15.

* z.moldabekov@hzdr.de

† a.cangi@hzdr.de

- [1] F. Graziani, M. P. Desjarlais, R. Redmer, and S. B. Trickey, *Frontiers and Challenges in Warm Dense Matter* (Springer, 2014).
- [2] CC. Chien, S. Peotta, and M. Di Ventra, “Quantum transport in ultracold atoms,” *Nature Phys.* **11**, 998–1004 (2015).

- [3] U. Schneider, L. Hackermüller, J. Ronzheimer, S. Will, S. Braun, T. Best, I. Bloch, E. Demler, S. Mandt, D. Rasch, and A. Rosch, “Fermionic transport and out-of-equilibrium dynamics in a homogeneous hubbard model with ultracold atoms,” *Nature Phys.* **8**, 213–218 (2012).
- [4] Claudio Giannetti, Massimo Capone, Daniele Fausti, Michele Fabrizio, Fulvio Parmigiani, and Dragan Mihailovic, “Ultrafast optical spectroscopy of strongly correlated materials and high-temperature superconductors: a non-equilibrium approach,” *Advances in Physics* **65**, 58–238 (2016).
- [5] Emanuel Gull, Andrew J. Millis, Alexander I. Lichtenstein, Alexey N. Rubtsov, Matthias Troyer, and Philipp Werner, “Continuous-time monte carlo methods for quantum impurity models,” *Rev. Mod. Phys.* **83**, 349–404 (2011).
- [6] Tobias Dornheim, Simon Groth, and Michael Bonitz, “The uniform electron gas at warm dense matter conditions,” *Phys. Rep.* **744**, 1 – 86 (2018).
- [7] P. Hohenberg and W. Kohn, “Inhomogeneous electron gas,” *Phys. Rev.* **136**, B864–B871 (1964).
- [8] Erich Runge and E. K. U. Gross, “Density-functional theory for time-dependent systems,” *Phys. Rev. Lett.* **52**, 997–1000 (1984).
- [9] N. Schlünzen, S. Hermanns, M. Bonitz, and C. Verdozzi, “Dynamics of strongly correlated fermions: *Ab initio* results for two and three dimensions,” *Phys. Rev. B* **93**, 035107 (2016).
- [10] Niclas Schlünzen, Sebastian Hermanns, Miriam Scharnke, and Michael Bonitz, “Ultrafast dynamics of strongly correlated fermions – Nonequilibrium Green functions and selfenergy approximations,” *Journal of Physics: Condensed Matter* **32**, 103001 (2020).
- [11] N. Schlünzen, J.-P. Joost, F. Heidrich-Meisner, and M. Bonitz, “Nonequilibrium dynamics in the one-dimensional Fermi-Hubbard model: Comparison of the nonequilibrium Green-functions approach and the density matrix renormalization group method,” *Phys. Rev. B* **95**, 165139 (2017).
- [12] M. Troyer and U. J. Wiese, “Computational complexity and fundamental limitations to fermionic quantum Monte Carlo simulations,” *Phys. Rev. Lett.* **94**, 170201 (2005).
- [13] T. Dornheim, “Fermion sign problem in path integral Monte Carlo simulations: Quantum dots, ultracold atoms, and warm dense matter,” *Phys. Rev. E* **100**, 023307 (2019).
- [14] M. Bonitz, T. Dornheim, Zh. A. Moldabekov, S. Zhang, P. Hamann, H. Kählert, A. Filinov, K. Ramakrishna, and J. Vorberger, “Ab initio simulation of warm dense matter,” *Physics of Plasmas* **27**, 042710 (2020).
- [15] B. Larder, D. O. Gericke, S. Richardson, P. Mabey, T. G. White, and G. Gregori, “Fast nonadiabatic dynamics of many-body quantum systems,” *Science Advances* **5** (2019), 10.1126/sciadv.aaw1634.
- [16] Zh. A. Moldabekov, M. Bonitz, and T. S. Ramazanov, “Theoretical foundations of quantum hydrodynamics for plasmas,” *Phys. Plasmas* **25**, 031903 (2018).
- [17] Diaw A. and Murillo M.S., “A viscous quantum hydrodynamics model based on dynamic density functional theory,” *Sci. Reports* **7**, 15352 (2017).
- [18] M. Bonitz, Zh. A. Moldabekov, and T. S. Ramazanov, “Quantum hydrodynamics for plasmas—quo

- vadis?" *Physics of Plasmas* **26**, 090601 (2019).
- [19] James Dufty, Kai Luo, and Jeffrey Wrighton, "Generalized hydrodynamics revisited," *Phys. Rev. Research* **2**, 023036 (2020).
 - [20] Alexander J. White, Ondrej Certik, Y. H. Ding, S. X. Hu, and Lee A. Collins, "Time-dependent orbital-free density functional theory for electronic stopping power: Comparison to the mermin-kohn-sham theory at high temperatures," *Phys. Rev. B* **98**, 144302 (2018).
 - [21] Y. H. Ding, A. J. White, S. X. Hu, O. Certik, and L. A. Collins, "Ab initio studies on the stopping power of warm dense matter with time-dependent orbital-free density functional theory," *Phys. Rev. Lett.* **121**, 145001 (2018).
 - [22] Rémi Goerlich, Giovanni Manfredi, Paul-Antoine Hervieux, Laurent Mertz, and Cyriaque Genet, "Probing quantum effects with classical stochastic analogs," (2020), [arXiv:2012.07120 \[quant-ph\]](https://arxiv.org/abs/2012.07120).
 - [23] P. K. Shukla and B. Eliasson, "Colloquium: Nonlinear collective interactions in quantum plasmas with degenerate electron fluids," *Rev. Mod. Phys.* **83**, 885–906 (2011).
 - [24] Padma K Shukla and B Eliasson, "Nonlinear aspects of quantum plasma physics," *Physics-Uspekhi* **53**, 51–76 (2010).
 - [25] Federico De Luca, Michele Ortolani, and Cristian Ciraci, "Free electron nonlinearities in heavily doped semiconductors plasmonics," *Phys. Rev. B* **103**, 115305 (2021).
 - [26] Muhammad Khalid, Fabio Della Sala, and Cristian Ciraci, "Optical properties of plasmonic core-shell nanomaterials: a quantum hydrodynamic analysis," *Opt. Express* **26**, 17322–17334 (2018).
 - [27] Muhammad Khalid and Cristian Ciraci, "Numerical analysis of nonlocal optical response of metallic nanoshells," *Photonics* **6** (2019), 10.3390/photonics6020039.
 - [28] Giovanni Manfredi, Paul-Antoine Hervieux, and Fatema Tanjia, "Quantum hydrodynamics for nanoplasmonics," in *Plasmonics: Design, Materials, Fabrication, Characterization, and Applications XVI*, Vol. 10722, edited by Din Ping Tsai and Takuo Tanaka, International Society for Optics and Photonics (SPIE, 2018) pp. 12 – 16.
 - [29] Cristian Ciraci and Fabio Della Sala, "Quantum hydrodynamic theory for plasmonics: Impact of the electron density tail," *Phys. Rev. B* **93**, 205405 (2016).
 - [30] S. Ali, H. Terças, and J. T. Mendonça, "Nonlocal plasmon excitation in metallic nanostructures," *Phys. Rev. B* **83**, 153401 (2011).
 - [31] D. I. Palade, "Nonlocal orbital-free kinetic pressure tensors for the fermi gas," *Phys. Rev. B* **98**, 245401 (2018).
 - [32] Cristian Ciraci, "Current-dependent potential for nonlocal absorption in quantum hydrodynamic theory," *Phys. Rev. B* **95**, 245434 (2017).
 - [33] G. Toscano, J. Straubel, A. Kwiatkowski, C. Rockstuhl, F. Evers, H. Xu, N. A. Mortensen, and M. Wubs, "Resonance shifts and spill-out effects in self-consistent hydrodynamic nanoplasmonics," *Nat. Communications* **6**, 7132 (2015).
 - [34] G. Manfredi and F. Haas, "Self-consistent fluid model for a quantum electron gas," *Phys. Rev. B* **64**, 075316 (2001).
 - [35] N. Crouseilles, P.-A. Hervieux, and G. Manfredi, "Quantum hydrodynamic model for the nonlinear electron dynamics in thin metal films," *Phys. Rev. B* **78**, 155412 (2008).
 - [36] Degond P., Mehats, F., and Ringhofer C., "Quantum energy-transport and drift-diffusion models," *J Stat Phys* **118**, 625–667 (2020).
 - [37] René Pinnau, "A review on the quantum drift diffusion model," *Transport Theory and Statistical Physics* **31**, 367–395 (2002).
 - [38] Robert E. Wyatt, *Quantum Dynamics with Trajectories Introduction to Quantum Hydrodynamics*, Interdisciplinary Applied Mathematics, Vol. 28 (Springer-Verlag New York, 2005).
 - [39] Arnaldo Donoso and Craig C. Martens, "Quantum tunneling using entangled classical trajectories," *Phys. Rev. Lett.* **87**, 223202 (2001).
 - [40] G. Gregori, B. Reville, and B. Larder, "Modified friedmann equations via conformal bohm-de broglie gravity," *The Astrophysical Journal* **886**, 50 (2019).
 - [41] Michael J. W. Hall, Dirk-André Deckert, and Howard M. Wiseman, "Quantum phenomena modeled by interactions between many classical worlds," *Phys. Rev. X* **4**, 041013 (2014).
 - [42] Carlos Castro Perelman, "Bohm's potential, classical/quantum duality and repulsive gravity," *Physics Letters B* **788**, 546 – 551 (2019).
 - [43] Kamel Ourabah, "Quasiequilibrium self-gravitating systems," *Phys. Rev. D* **102**, 043017 (2020).
 - [44] Kamel Ourabah, "Linear dark matter density perturbations: A wigner approach," *EPL (Europhysics Letters)* **132**, 19002 (2020).
 - [45] Alvaro Navarrete, Angel Paredes, José R. Salgueiro, and Humberto Michinel, "Spatial solitons in thermo-optical media from the nonlinear schrödinger-poisson equation and dark-matter analogs," *Phys. Rev. A* **95**, 013844 (2017).
 - [46] Pedro F. González-Díaz, "Subquantum dark energy," *Phys. Rev. D* **69**, 103512 (2004).
 - [47] G. Manfredi, "How to model quantum plasmas," *Fields Inst. Commun.* **46**, 263–287 (2005).
 - [48] Tobias Dornheim, Jan Vorberger, and Michael Bonitz, "Nonlinear electronic density response in warm dense matter," *Phys. Rev. Lett.* **125**, 085001 (2020).
 - [49] L. B. Fletcher, H. J. Lee, T. Döppner, E. Galtier, B. Nagler, P. Heimann, C. Fortmann, S. LePape, T. Ma, M. Millot, A. Pak, D. Turnbull, D. A. Chapman, D. O. Gericke, J. Vorberger, T. White, G. Gregori, M. Wei, B. Barbel, R. W. Falcone, C.-C. Kao, H. Nuhn, J. Welch, U. Zastrau, P. Neumayer, J. B. Hastings, and S. H. Glenzer, "Ultrabright x-ray laser scattering for dynamic warm dense matter physics," *Nature Photonics* **9**, 274–279 (2015).
 - [50] U. Zastrau, P. Sperling, M. Harmand, A. Becker, T. Bornath, R. Bredow, S. Dziarzhytski, T. Fennel, L. B. Fletcher, E. Förster, S. Göde, G. Gregori, V. Hilbert, D. Hochhaus, B. Holst, T. Laarmann, H. J. Lee, T. Ma, J. P. Mithen, R. Mitzner, C. D. Murphy, M. Nakatsutsumi, P. Neumayer, A. Przystawik, S. Roling, M. Schulz, B. Siemer, S. Skruszewicz, J. Tiggesbäumker, S. Toleikis, T. Tschentscher, T. White, M. Wöstmann, H. Zacharias, T. Döppner, S. H. Glenzer, and R. Redmer, "Resolving ultrafast heating of dense cryogenic hydrogen," *Phys. Rev. Lett.* **112**, 105002 (2014).
 - [51] B. K. Ofori-Okai, M. C. Hoffmann, A. H. Reid, S. Edstrom, R. K. Jobe, R. K. Li, E. M. Mannebach, S. J. Park, W. Polzin, X. Shen, S. P. Weathersby, J. Yang, Q. Zheng, M. Zajac, A. M. Lindenberg, S. H. Glenzer, and X. J. Wang, "A terahertz pump mega-electron-volt ultrafast electron diffraction probe apparatus at the SLAC accel-

- erator structure test area facility,” *J. Inst* **13**, P06014–P06014 (2018).
- [52] E. Goulielmakis, M. Uiberacker, R. Kienberger, A. Baltuska, V. Yakovlev, A. Scrinzi, T. Westerwalbesloh, U. Kleineberg, U. Heinzmann, M. Drescher, and F. Krausz, “Direct measurement of light waves,” *Science* **305**, 1267–1269 (2004).
- [53] U. Fröhling, M. Wieland, M. Gensch, T. Gebert, B. Schütte, M. Krikunova, R. Kalms, F. Budzyn, O. Grimm, J. Rossbach, E. Plönjes, and M. Drescher, “Single-shot terahertz-field-driven x-ray streak camera,” *Nature Photonics* **3**, 523 (2009).
- [54] A. K. Kazansky, I. P. Sazhina, and N. M. Kabachnik, “Angular streaking of auger-electrons by THz field,” *J. Phys. B: Atomic, Mol. and Opt. Phys* **52**, 045601 (2019).
- [55] R. Helled, G. Mazzola, and R. Redmer, “Understanding dense hydrogen at planetary conditions,” *Nat. Rev. Phys.* **2**, 562–574 (2020).
- [56] Boris Yu. Sharkov, Dieter H.H. Hoffmann, Alexander A. Golubev, and Yongtao Zhao, “High energy density physics with intense ion beams,” *Matter and Radiation at Extremes* **1**, 28–47 (2016).
- [57] E Madelung, “Quantentheorie in hydrodynamischer Formulierung,” *Z. Physik* **40** (1927).
- [58] David Bohm, “A suggested interpretation of the quantum theory in terms of “hidden” variables. i,” *Phys. Rev.* **85**, 166–179 (1952).
- [59] D Bohm, B.J Hiley, and P.N Kaloyerou, “An ontological basis for the quantum theory,” *Physics Reports* **144**, 321–375 (1987).
- [60] W. Kohn and L. J. Sham, “Self-Consistent Equations Including Exchange and Correlation Effects,” *Phys. Rev.* **140**, A1133–A1138 (1965).
- [61] *Supplemental material*, Tech. Rep.
- [62] M. Lazar, P. K. Shukla, and A. Smolyakov, “Surface waves on a quantum plasma half-space,” *Physics of Plasmas* **14**, 124501 (2007).
- [63] S. X. Hu, B. Militzer, V. N. Goncharov, and S. Skupsky, “Strong coupling and degeneracy effects in inertial confinement fusion implosions,” *Phys. Rev. Lett.* **104**, 235003 (2010).
- [64] O.L. Landen, S.H. Glenzer, M.J. Edwards, R.W. Lee, G.W. Collins, R.C. Cauble, W.W. Hsing, and B.A. Hammel, “Dense matter characterization by x-ray thomson scattering,” *Journal of Quantitative Spectroscopy and Radiative Transfer* **71**, 465–478 (2001).
- [65] T. Ma, T. Döppner, R. W. Falcone, L. Fletcher, C. Fortmann, D. O. Gericke, O. L. Landen, H. J. Lee, A. Pak, J. Vorberger, K. Wünsch, and S. H. Glenzer, “X-ray scattering measurements of strong ion-ion correlations in shock-compressed aluminum,” *Phys. Rev. Lett.* **110**, 065001 (2013).
- [66] Tobias Dornheim, Simon Groth, Jan Vorberger, and Michael Bonitz, “Permutation-blocking path-integral Monte Carlo approach to the static density response of the warm dense electron gas,” *Phys. Rev. E* **96**, 023203 (2017).
- [67] Jianwei Sun, Adrienn Ruzsinszky, and John P. Perdew, “Strongly constrained and appropriately normed semilocal density functional,” *Phys. Rev. Lett.* **115**, 036402 (2015).
- [68] E. I. Moses, R. N. Boyd, B. A. Remington, C. J. Keane, and R. Al-Ayat, “The National Ignition Facility: Ushering in a new age for high energy density science,” *Phys. Plasmas* **16**, 041006 (2009).
- [69] M. Keith Matzen, M. A. Sweeney, R. G. Adams, J. R. Asay, J. E. Bailey, G. R. Bennett, D. E. Bliss, D. D. Bloomquist, T. A. Brunner, R. B. Campbell, G. A. Chandler, C. A. Coverdale, M. E. Cuneo, J.-P. Davis, C. Deeney, M. P. Desjarlais, G. L. Donovan, C. J. Garasi, T. A. Haill, C. A. Hall, D. L. Hanson, M. J. Hurst, B. Jones, M. D. Knudson, R. J. Leeper, R. W. Lemke, M. G. Mazarakis, D. H. McDaniel, T. A. Mehlhorn, T. J. Nash, C. L. Olson, J. L. Porter, P. K. Rambo, S. E. Rosenthal, G. A. Rochau, L. E. Ruggles, C. L. Ruiz, T. W. L. Sanford, J. F. Seamen, D. B. Sinars, S. A. Slutz, I. C. Smith, K. W. Struve, W. A. Stygar, R. A. Vesey, E. A. Weinbrecht, D. F. Wenger, and E. P. Yu, “Pulsed-power-driven high energy density phys. and inertial confinement fusion research,” *Phys. Plasmas* **12**, 055503 (2005).
- [70] O. A. Hurricane, D. A. Callahan, D. T. Casey, E. L. Dewald, T. R. Dittrich, T. Döppner, S. Haan, D. E. Hinkel, L. F. Berzak Hopkins, O. Jones, A. L. Kritcher, S. Le Pape, T. Ma, A. G. MacPhee, J. L. Milovich, J. Moody, A. Pak, H.-S. Park, P. K. Patel, J. E. Ralph, H. F. Robey, J. S. Ross, J. D. Salmonson, B. K. Spears, P. T. Springer, R. Tommasini, F. Albert, L. R. Benedetti, R. Bionta, E. Bond, D. K. Bradley, J. Caggiano, P. M. Celliers, C. Cerjan, J. A. Church, R. Dylla-Spears, D. Edgell, M. J. Edwards, D. Fittinghoff, M. A. Barrios Garcia, A. Hamza, R. Hatarik, H. Herrmann, M. Hohenberger, D. Hoover, J. L. Kline, G. Kyrala, B. Koziowski, G. Grim, J. E. Field, J. Frenje, N. Izumi, M. Gatu Johnson, S. F. Khan, J. Knauer, T. Kohut, O. Landen, F. Merrill, P. Michel, A. Moore, S. R. Nagel, A. Nikroo, T. Parham, R. R. Rygg, D. Sayre, M. Schneider, D. Shaughnessy, D. Strozzi, R. P. J. Town, D. Turnbull, P. Volegov, A. Wan, K. Widmann, C. Wilde, and C. Yeaman, “Inertially confined fusion plasmas dominated by alpha-particle self-heating,” *Nat. Phys.* **12**, 800–806 (2016).
- [71] Eugenio Cocchi, Luke A. Miller, Jan H. Drewes, Marco Koschorreck, Daniel Pertot, Ferdinand Brennecke, and Michael Köhl, “Equation of state of the two-dimensional hubbard model,” *Phys. Rev. Lett.* **116**, 175301 (2016).
- [72] J. Austin Ellis, Attila Cangi, Normand A. Modine, J. Adam Stephens, Aidan P. Thompson, and Sivasankaran Rajamanickam, “Accelerating finite-temperature kohn-sham density functional theory with deep neural networks,” (2020), [arXiv:2010.04905 \[cond-mat.mtrl-sci\]](https://arxiv.org/abs/2010.04905).
- [73] F. Brockherde, L. Li, K. Burke, and K. Müller, “Bypassing the kohn-sham equations with machine learning,” *Nature Communications* **8** (2017).
- [74] T. Dornheim, J. Vorberger, S. Groth, N. Hoffmann, Zh.A. Moldabekov, and M. Bonitz, “The static local field correction of the warm dense electron gas: An ab initio path integral Monte Carlo study and machine learning representation,” *J. Chem. Phys* **151**, 194104 (2019).
- [75] Tobias Dornheim, Attila Cangi, Kushal Ramakrishna, Maximilian Böhme, Shigenori Tanaka, and Jan Vorberger, “Effective static approximation: A fast and reliable tool for warm-dense matter theory,” *Phys. Rev. Lett.* **125**, 235001 (2020).
- [76] de Broglie L., *Nonlinear wave mechanics: A causal interpretation* (Elsevier, Amsterdam, 1960).

- [77] Ali Shojai and Fatimah Shojai, “About some problems raised by the relativistic form of de-broglie–bohm theory of pilot wave,” *Physica Scripta* **64**, 413 (2006).